Improved tabletability after a polymorphic transition of delta-mannitol during twin screw granulation

V.Vanhoorne[1], B. Bekaert[1], E. Peeters[2], T. De Beer[2], J-P. Remon[1], C. Vervaet[1]

[1]Laboratory of Pharmaceutical Technology, Ghent University (Belgium)

[2]Laboratory of Pharmaceutical Process Analytical Technology, Ghent University (Belgium)

Corresponding Author:

Chris Vervaet

Ghent University

Laboratory of Pharmaceutical Technology

Ottergemsesteenweg 460

9000 Ghent

Belgium

Tel: +32 9 264 80 69

Fax: +32 9 222 82 36

E-mail: Chris.Vervaet@UGent.be

Abstract

In most formulations processed via continuous twin screw granulation microcrystalline cellulose (MCC) and/or lactose are used as excipients, but mannitol is also a preferred excipient for wet granulation and tableting due to its non-hygroscopicity and inertness. Therefore, the aim of the current study was to investigate the influence of process parameters on critical quality attributes of granules (moisture content, solid state, morphology, size distribution, specific surface area, friability, flowability and hygroscopicity) and tablets (tensile strength and friability) after twin screw granulation of δ-mannitol. The δ-polymorph was selected since a moisture-induced transformation to β-mannitol was observed during batch wet granulation, which exhibited a unique morphology with a large surface area and improved tabletability. A full factorial experimental design was performed, varying screw speed (400 - 900 rpm), granulation temperature (25 - 40 °C), number of kneading elements (6 or 12) and liquid-to-solid (L/S) ratio, on the granulation unit of a ConsiGma™-25 line (a continuous powder-to-tablet manufacturing system). After tray drying the granules were milled and tableted. The results showed that the polymorphic transition from δ- to β-mannitol also occurred during twin screw granulation, although the residence time and L/S ratios were much lower in continuous twin screw granulation compared to batch processing. However, the polymorphic transition was not complete in all experiments and depended on the L/S ratio, screw speed and number of kneading elements. Nevertheless all granules exhibited the unique morphology linked to the polymorphic transition and had a superior tabletability compared to granules produced with β-mannitol as starting material. This was attributed to enhanced plastic deformation of the granules manufactured using δ-mannitol as starting material. In addition, it was concluded that mannitol was granulated via a different mechanism than other, less-soluble, excipients (e.g. lactose, microcrystalline cellulose) due to its high solubility and dissolution rate as the influence of process parameters on the mannitol granule characteristics was different.

KEYWORDS: δ-mannitol, Polymorphism, Tabletability, Continuous production, Twin screw granulation, Plastic deformability

List of abbreviations

C%	Compressibility index
d_{50}	Median particle size
E	Energy
ffc	Flowability index
IER	In-die elastic recovery
L/S	Liquid-to-solid
LOD	Loss on drying
MCC	Microcrystalline cellulose
MCP	Main compression pressure
PC	Plasticity constant
PCA	Principal component analysis
PVP	Polyvinylpyrrolidone
RH	Relative humidity
RMSECV	Root mean square error of cross validation
SEM	Scanning electron microscopy
T_a	Tablet height immediately after ejection
T_{id}	Tablet height under maximum compression force
V_0	Bulk volume
V_{1250}	Tapped volume
XRD	X-ray diffraction

1. Introduction

The interest in twin screw granulation is growing as it is a continuous process that can be implemented into a fully continuous from-powder-to-tablet line. This concept offers economic advantages, improved product quality and a lower environmental impact of processing [1, 2, 3, 4]. Moreover regulatory authorities recently recognized the potential of continuous manufacturing and encouraged adoption of it by the pharmaceutical industry [3].

Only a limited number of studies on twin screw granulation addressed formulation development while most studies focused on the influence of process parameters on granule quality [5, 6, 7, 8, 9, 10, 11, 12, 13, 14, 15, 16, 17, 18, 19, 20]. Moreover, most studies used formulations with lactose or microcrystalline cellulose as fillers. Mannitol is a preferred excipient for the formulation of tablets due to its non-hygroscopic character, compatibility with primary amines, high sweetness, cooling mouth sensation, high solubility and fast disintegration [21, 22, 23, 24]. Although it is a frequently used tablet diluent in the neutraceutical and pharmaceutical industry, no literature reports about the use of mannitol as an excipient during twin screw granulation are available [23].

Three polymorphs of mannitol have been described: α-, β- and δ-mannitol. However, most commercially available mannitol grades consist of α- or β-mannitol or mixtures thereof. During high shear granulation of δ-mannitol a moisture mediated polymorphic transition from δ- to β-mannitol was reported which resulted in a unique granule morphology with a high specific surface area and enhanced plastic deformability [22]. As a result the δ-polymorph of mannitol (commercialized as Parteck Delta M by Merck) is specifically promoted for wet granulation processes to take advantage of the improved tableting properties associated with the moisture-induced polymorphic transition from δ- to β-mannitol during wet granulation [25].

It was our aim to use δ-mannitol during a continuous wet granulation process using a twin screw granulator and to evaluate how process parameters (number of kneading elements, granulation temperature, screw speed, liquid-to solid (L/S) ratio) affected the critical quality attributes of granules and tablets. In addition, it was investigated if the polymorphic transition from δ- to β-mannitol, which has only been reported during batch high shear granulation, also occurred during twin screw granulation and whether this transition depended on process parameters as the residence time as well as the liquid content during twin-screw granulation are considerably lower compared to batch granulation processes [6, 14, 17, 19, 26, 27, 28, 29].

2. Materials and methods

2.1. Materials

δ-mannitol (Parteck® Delta M), β-mannitol (C*PharmMannidex 16700) and α-mannitol (Pearlitol 200) were kindly donated by Merck Millipore (Darmstadt, Germany), Cargill Italy (Castelmassa, Italy) and Cargill Belgium (Vilvoorde, Belgium), respectively. These samples were used as reference materials. Distilled water was used as granulation liquid. Magnesium stearate (Fagron, Waregem, Belgium) was used as lubricant for tableting. Raman spectra of reference materials of α-, β- and δ-mannitol were adopted from De Beer et al. [30].

2.2. Methods

2.2.1. Preparation granules

Pure β- or δ-mannitol was added to the loss-in-weight feeder (KT20, K-Tron Soder, Niederlenz, Switzerland) of the ConsiGma™-25 system (GEA Pharma Systems Collette™, Wommelgem, Belgium). In this continuous oral solid dosage manufacturing line a twin screw granulator is directly connected to a six-segmented fluid bed dryer, a mill and finally a tablet press. The barrel of the twin screw granulator (length-to-diameter ratio: 20:1) can be divided into a feed segment with conveying elements and a work segment where the powder is intensively mixed with granulation liquid by kneading elements. Water as granulation liquid was pumped into the barrel just before the first kneading element via a double liquid addition port, injecting granulation liquid on top of each screw. The equipment has an in-built torque gauge which monitors the torque at 1-second intervals. The torque values obtained after equilibrium of the process were averaged to give the overall torque during each run. A PT-100 temperature sensor was integrated in the work segment of the barrel and linked to a feedback control system which regulates the temperature in the barrel jacket and compensates for temperature increase during the process due to friction. As the aim of the study was to evaluate the polymorphic transition of δ-mannitol during granulation, the fluid bed dryer was not used to avoid interference of dynamic drying on the product properties. The granules were collected after the granulation unit and oven dried at 40 °C for 24 h until the moisture content (as measured by loss on drying (LOD)) was below 1%. After drying, 800 g

of the granules was milled through a 1500 µm grater screen with square impeller at 900 rpm using the comill (U10, Quadro, Ontario, Canada) incorporated in the ConsiGma™-25 line.

2.2.2. Design of experiments

A full factorial experimental design (20 runs) including four process parameters was performed using pure δ-mannitol: L/S ratio (0.08 – 0.16), barrel temperature (25 – 40 °C), screw speed (400 – 900 rpm), number of kneading elements (6 or 12). The throughput was fixed at 20 kg/h in all experiments. The screw configuration with 6 kneading elements consisted of 1 block of kneading elements whereas the screw configuration with 12 kneading elements consisted of 2 kneading zones of 6 kneading elements (2x6) separated by a conveying zone. Reference is made to these configurations as 1x6 and 2x6, respectively. For both screw configurations the distance between liquid addition and the first kneading element was kept constant. Two center points (with screw configurations 1x6 and 2x6) were run in duplicate. An overview of the experiments is given in Table 1. The results were analyzed using Modde 10.1 (Umetrics, Umeå, Sweden) software. As the applied design was a full factorial design, interactions could be detected. However, the statistically non-significant interactions were not shown in the effect plots throughout the paper.

Additionally two granulation experiments (runs 21 and 22) were performed with pure β-mannitol to allow comparison with the granules prepared with pure δ-mannitol (Table 1).

2.2.3. Preparation of tablets

The milled granules (runs 1 - 22) and β- and δ-mannitol starting material were blended with 1.5% magnesium stearate in a tumbling blender for 3 minutes (T2F, W.A. Bachofen, Basel, Switzerland) before tableting. Tablets were prepared in manual mode at a speed of 20 tablets per minute on the Modul™ P tablet press (GEA Pharma Systems Courtoy™, Halle, Belgium) part of the ConsiGma™-25 line. The press was equipped with 1 pair of round flat-faced bevel-edged Euro B punches (GEA Pharma Systems, Halle, Belgium) (diameter 10 mm) and an overfill cam of 12 mm. A single-paddle feed frame equipped with a paddle with round thin fingers (n = 8) rotating counter-clockwise at 20 rotations per minute (rpm) (GEA Pharma Systems, Halle, Belgium) was used. This setup allowed producing tablets on a rotary press with a minimal amount of granules (± 50 g). Tablets were compressed at 3

different main compression pressures (MCP): 150, 250 and 350 MPa, for assessment of their tabletability. Tablets compressed at 350 MPa were selected for friability testing.

To elucidate the bonding mechanisms during compression, tableting experiments were performed with monitoring of punch stroke movements by linear variable displacement transducers clamped on the pair of punches (GEA Pharma Systems, Halle, Belgium). Data from these sensors was acquired continuously and transmitted wireless to a data acquisition and data analysis system (CDAAS, GEA Pharma Systems, Halle, Belgium). The CDAAS system measured signals (pre- and main compression force and displacement, punch strokes) and allowed reviewing and analysis of the recorded data. From the punch stroke signals, in-die elastic recovery (IER) and energy plots were calculated. For each formulation the punch stroke movements were monitored during compression at 150 MPa.

2.2.4. Evaluation of the granules

2.2.4.1. Loss on drying

The residual moisture content of the granules was determined via LOD using a moisture analyzer (Mettler LP16, Mettler-Toledo, Zaventem, Belgium) including an infrared dryer and a balance. A sample of 5 g was dried at 105 °C until the weight was constant for 30 s.

2.2.4.2. Solid state characterization

Raman spectra (Rxn1, Kaiser Optical Systems, Ann Arbor, USA) of the reference materials, unmilled (runs 1 – 22) and milled granules (runs 1 – 20) were recorded using exposure times of 10 s with 3 accumulations. Additionally, unmilled granules were measured after 6 months storage at 40 °C and 75% relative humidity (RH) and at 25 °C and 40% RH. At least 5 spectra were recorded for each sample. For the tablets, one spectrum was collected at each compression pressure. A PLS model was constructed to determine the ratio of δ- and β-mannitol in the granulated samples (Simca 13.0.3 software, Umetrics, Umeå, Sweden). This model was developed from the Raman spectra (5 spectra for each calibration sample) of calibration samples (i.e., powder mixtures) with a ratio of δ-mannitol:β-mannitol varying between 0-100% with increments of 10%. Data were corrected by standard

normal variate preprocessing and center-scaled prior to analysis. Standard Normal Variate preprocessing was applied to eliminate the additive baseline offset variations and multiplicative scaling effects in the spectra which may be caused by small variations in distance between the Raman probe and the sample and possible differences in product density. The results of the PLS analysis were averaged for each sample.

Additionally, XRD was performed on the reference materials and unmilled granules on a CuKα diffractor (ARL™ X'TRA, Thermo Fischer Scientific, Waltham, United States) with a voltage of 40 mV in the angular range of 8 ° < 2θ < 60 ° using a step scan mode with step size of 0.02 ° and counting time of 1 s / step.

2.2.4.3. Morphology

The unmilled granules and reference materials of β- and δ-mannitol were examined by scanning electron microscopy (SEM) (FEI QuantaTM 200F, FEI, Hillsboro, USA) after sputtering with a gold coating (Emitech SC7620, Quorum Technologies, East Grinstead, UK) to improve the electron conductivity of the samples.

2.2.4.4. Particle size analysis

Granule size was analyzed before and after milling via dynamic image analysis using the QICPIC™ system (Sympatec, Clausthal-Zellerfeld, Germany) equipped with a vibrating feeder system (Vibri/L™) for gravimetrical feeding of the granules. Samples of 20 g were measured in duplicate. Windox 5 software (Sympatec, Clausthal-Zellerfeld, Germany) was used to calculate the median granule size (d_{50}) as the equivalent projected circle diameter based on a volume distribution. The amounts of fines and oversized granules were defined as the fractions <150 µm and >1500 µm, respectively. The yield of the process was defined as the percentage of granules between 150 and 1500 µm.

2.2.4.5. Flowability testing

The flowability expressed as the flowability index (ffc) of the milled granules was measured in duplicate by ring shear testing (Type RST-XS, Dietmar Schulze

Schüttgutmesstechnik, Wolfenbuttel, Germany). The powders were tested using three consolidation stresses, 400, 600 and 800 Pa, at a preshear of 1000 Pa.

Additionally, the compressibility index (C%) was calculated from the bulk and tapped densities of the milled granules. The bulk volume (V_0) of 30 g milled granules was measured in a 100 ml graduated cylinder as well as the tapped volume after 1250 taps (V_{1250}) in a tapping machine (J. Englesman, Ludwigshafen, Germany). Experiments were performed in duplicate. Bulk and tapped densities were calculated as 30 g/V_0 and 30 g/V_{1250}, respectively. The compressibility index was calculated from the bulk (ρ_i) and tapped (ρ_f) densities using the following equation: $C\% = [(\rho_f - \rho_i)/ \rho_f]*100$.

2.2.4.6. Friability analysis

The granule friability was determined in duplicate using a friabilator (PTF E Pharma Test, Hainburg, Germany) at a speed of 25 rpm for 10 min, by subjecting 10 g (I_{wt}) of milled granules together with 200 glass beads (mean diameter 4 mm) to falling shocks. Prior to determination, the granule fraction <250 µm was removed to assure the same starting conditions. Afterwards, the glass beads were removed and the weight retained on a 250 µm sieve (F_{wt}) was determined. The friability was calculated as $[(I_{wt} – F_{wt})/I_{wt}]*100$.

2.2.4.7. Dynamic vapor sorption (DVS)

Dynamic vapor sorption (DVS Advantage, Surface Measurement Systems, Middlesex, UK) was used to assess the overall hygroscopicity of the materials. Approximately 10 – 20 mg of unmilled sample was placed into the instrument's microbalance and dried by a stream of dry nitrogen at 25 °C until equilibrium (i.e. a weight change of less than 0.002% per min during at least 15 min). The samples were subsequently exposed to varying RH, 0, 20, 40, 60, 80, 90 and 95% and equilibrated at each interval. Sorption and desorption of the samples were recorded at these RH conditions.

2.2.4.8. Specific surface area analysis

Nitrogen adsorption measurements were performed at 77 K on a selection of unmilled granules and β- and δ-mannitol reference material using a TriStar 3000 gas

sorption apparatus (Micromeritics Inc., Norcross, USA). The specific surface area of the powder samples was determined from the adsorption isotherm using the Brunauer-Emmett-Teller–theory.

2.2.5. Evaluation of the tablets

The hardness, thickness and diameter of the tablets (n = 10) were determined using a hardness tester (Type HT 10, Sotax, Basel, Switzerland) and the tensile strength (TS) of the tablets was calculated according to the formula of Fell and Newton [31]: $T = 2F/\pi dt$

Where F, d and t denote the diametral crushing force, tablet diameter and tablet thickness, respectively.

The tablet friability was determined using a friabilator (PTFE, Pharma Test, Hainburg, Germany) as described in the European Pharmacopeia at a speed of 25 rpm for 4 min. The percentage weight loss was expressed as the tablet friability.

Energy plots were calculated based on the punch stroke movements. In the energy plot the punch stroke is plotted against the compression force. An example of an energy plot is shown in Figure 1 where B is the punch stroke when the punch force is zero, C is the punch stroke when the punch force is maximal (A) and D is punch stroke after decompression when punch force is zero again. The areas of ABC, ABD and ADC show the total compression energy, plastic energy and elastic energy, respectively [22]. Based on the energy plot, the plasticity constant (PC) was calculated as: plastic energy/total compression energy*100. This parameter expresses the plasticity of a material under deformation.

The in-die elastic recovery (IER) was calculated using the Armstrong and Haines-Nutt equation:

$IER = (T_a – T_{id}) / T_{id} * 100,$

where T_a denotes the tablet height immediately after ejection and T_{id} the tablet height under maximum compression force [32].

3. Results and discussion

Although mannitol is a preferred excipient for wet granulation and tableting, its behavior during twin screw granulation was not studied yet. In contrast to frequently used excipients during twin screw granulation (lactose, MCC), mannitol exhibits a high solubility and solubility rate. Therefore mannitol was expected to behave differently during granulation. Moreover polymorphic transitions are possible during recrystallization of mannitol. Such transition of δ- to β-mannitol was reported during high shear granulation and promoted the tabletability of the granules. An experimental design was performed to investigate the influence of four process parameters on the process and critical quality attributes of mannitol granules and tablets.

3.1. Evaluation of the granulation process

The torque varied strongly across all experiments. Torque values as low as 0.9 - 1.0 Nm (runs 13 and 19) were recorded, whereas in runs 7 and 8 the torque exceeded 20 Nm, the maximal torque tolerated by the granulator. These runs were conducted with 12 kneading elements, at a low screw speed and using a high L/S ratio. Run 7 was excluded from the design as no material could be collected. During run 8 a limited amount of granules was collected after equilibration which allowed solid state characterization and size and shape analysis but no further characterization. A torque value of 20 Nm was assigned to this run in the experimental design. The influence of the granulation parameters on torque is shown in the effect plot in Figure 2.

The screw speed, which was varied over a broad range of 400 - 900 rpm in the current study, proved the major factor affecting torque. Since the throughput was constant in all experiments, increasing the screw speed resulted in a lower filling degree of the barrel which in turn yielded lower torque values. This is in accordance with research from Kumar et al., Tan et al., Tu et al. and Keleb et al. (on formulations with mainly lactose, microcrystalline cellulose (MCC) or paracetamol), but is opposed to the report of Vercruysse et al. (on a formulation with lactose and theophylline) stating that screw speed did not influence torque [5, 7, 17, 26, 29]. The influence of screw speed on torque is possibly formulation dependent, but could also be more prominent at lower screw speeds (and consequently higher filling degrees) since the research of Kumar et al. (500-900 rpm), Tan et al. (100-150 rpm) and current study (400-900 rpm) were conducted at lower screw speeds than the study of Vercruysse et al. (600-950 rpm).

Increasing the L/S ratio resulted in higher torque values. This is in agreement with research of Dhenge et al. (on a formulation with mainly lactose and MCC) who reported that a higher L/S ratio prolonged the residence time in the barrel as the material behaved like paste [27]. However, an inverse relationship between L/S ratio and torque was established by Tan et al. and Kumar et al. (on formulations with mainly paracetamol and lactose, respectively) [6, 17]. They explained that at a higher L/S ratio the material was more malleable, thus requiring less energy to deform and compress [17]. Finally, Tu et al. reported (on a formulation with MCC) that the torque increased until a critical L/S ratio was reached and then decreased with formation of over-wetted particles. The effect of the L/S ratio on torque appears again formulation dependent.

A higher number of kneading elements resulted in higher torque values due to the retaining character of the kneading elements causing more friction. Additionally, more mannitol could go into solution and participate in bond formation which could increase the torque. Varying the granulation temperature did not have a significant effect on torque.

3.2. Influence of the design variables on granule quality

3.2.1. Solid state characterization

Raman spectra of the unmilled and milled granules were compared to reference spectra of α-, β- and δ-mannitol. The data showed that a polymorphic transition occurred from δ- to β-mannitol during twin screw granulation, similar to the observations of Yoshinari et al. for batch granulation [22]. This is noteworthy since the residence time during twin screw granulation is short, typically 5 - 20 s, compared to batch granulation where granulation times are in the order of tens of minutes [6, 19, 26, 27, 32]. Moreover, Keleb et al., Beer et al. and Tan et al. demonstrated that lower L/S ratios are used in twin screw granulation in comparison to batch granulation [17, 28, 29]. The L/S ratio that could be applied during granulation in the current study varied between 0.08 and 0.16, whereas Yoshinari et al. used an L/S ratio of 0.25 during batch granulation [22]. However, the polymorphic transition was not complete in all samples of current study. Therefore a PLS model was constructed to quantify the percentage of δ-mannitol left in the samples. The model gave a rough quantitative estimation of the composition of the samples since its root mean square error of cross validation (RMSECV) was relatively high (8.15). As β-

and δ-mannitol particles where physically mixed in the PLS calibration samples, the variability on the spectra of these samples was higher than of the measured granules (where β- and δ-mannitol are homogeneously mixed during granulation), resulting in a model with a high RMSECV value. An overview of the percentage δ-mannitol in the granulated samples before and after milling is presented in Table 2 and it is clear that milling did not change the polymorphic content of the samples. Stability of δ-mannitol, although thermodynamically the least stable mannitol polymorph, under mechanical stress was also demonstrated by Burger et al. [34].

These results were also included as responses in the experimental design to investigate the influence of the process parameters on the polymorphic transition from δ- to β-mannitol. The corresponding effect plots showed that the L/S ratio, screw speed and number of kneading elements influenced the polymorphic transition during granulation and confirmed that milling did not significantly influence the polymorphic content (Figure 3). The L/S ratio was the strongest influencing process parameter as more mannitol could go into solution at higher L/S ratios [35]. More mannitol could go into solution at higher L/S ratios which favored recrystallization to the β-polymorph. Increasing the screw speed resulted in more residual δ-mannitol in the samples as it shortened the residence time and consequently also the duration of granulation during which the polymorphic transition could occur. Mixing of mannitol and water induced by the kneading elements also affected the polymorphic composition of the granulated samples. More kneading elements resulted in more β-mannitol as more mixing promoted mannitol to go into solution. Run 8, which was performed with a high L/S ratio, low screw speed and 12 kneading elements, yielded the sample with the lowest fraction of residual δ-mannitol. However, combining these process parameters was not feasible because of too high torque. In the section on tablet quality it will be investigated if complete transition of δ- to β-mannitol is necessary to obtain improved tablet properties.

The results of the Raman analysis were confirmed by XRD measurements (Figure 4). β-mannitol was identified in all samples by its unique peak at 14.74°. Moreover, a small peak at 9.90°, selective for δ-mannitol, in the diffractograms of runs 5, 12, 13, 18 and 19 indicated a significant residual percentage of δ-mannitol in these samples [21, 22, 30, 34, 36, 37]. The overall lower intensity of the peaks in the diffractograms of the granules was attributed to a different crystal habit of the granules in comparison to the reference materials (powders) [38].

3.2.2. Morphology and specific surface analysis

SEM images of the granulated samples were compared to those of β- and δ-mannitol reference materials. The granules derived from δ-mannitol as starting material (e.g. runs 14 and 19) possessed a completely different morphology than the granules derived from β-mannitol (runs 21 and 22) and the reference materials of β- and δ-mannitol (Figure 5). They consisted of aggregates of many small needle-shaped primary crystals, similarly as described by Yoshinari et al. after a polymorphic transition from δ- to β-mannitol during high shear granulation [22, 35]. This specific morphology was observed in all granules derived from δ-mannitol and was not correlated to the percentage of residual δ-mannitol in the granules.

Yoshinari et al. also reported on a higher specific surface area associated with this specific surface morphology. Therefore, the specific surface area (SSA) of a selection of granules was determined (Table 2). The SSA of the granules derived from δ-mannitol was at least twice the SSA of δ-mannitol reference material, at least 8 times the SSA of β-mannitol reference material and at least 4 times the SSA of granules derived from β-mannitol. This confirmed the microscopic observations.

3.2.3. Size analysis

The particle size distributions of granules before and after milling were determined. They were evaluated with regard to d_{50}, fines fraction (<150 µm), oversized fraction (>1500 µm) and yield (150-1500 µm).

A significant relationship between the L/S ratio and the d_{50}, fines fraction and oversized fraction was detected: by adding more water, more liquid and solid bonds were formed, resulting in a larger d_{50}, less fines and more oversized particles (Figure 6). This effect of L/S on particle size is generally recognized in literature [1, 5, 14, 19, 27].

A direct relationship was established between screw speed and the d_{50} and oversized fraction. This is in contrast to most literature reports (on a variety of formulations), indicating no correlation between screw speed and d_{50} [1, 7, 16, 17, 29] or an inverse relationship [1, 5, 8]. They attributed the larger particle size at lower screw speeds to higher torque values, resulting in higher compressive forces in the granulator barrel. However, it is clear from the effect plot in Figure 6 that the directly proportional relation was dominant for all size parameters in the current study. The solubility and the solubility rate of the formulation could be determining factors for the influence of screw speed on granule size. Pure mannitol was used as excipient in current study and has a higher solubility and solubility rate constant than most

other commonly used excipients for twin screw granulation (lactose, MCC, active drug substances…) [1, 7, 8, 10, 12, 13, 17, 19, 20, 26, 27, 39, 40]. Whereas higher compressive forces at low screw speed generally favor granule growth with less soluble excipients, granulation of mannitol could be driven by its high and fast solubility, rather than by compressive forces. It can even be concluded that compressive forces at low screw speeds induce breakage of the mannitol granules due to collision and friction. Additionally, an interaction between screw speed and L/S ratio influenced the d_{50} and oversized fraction: the positive influence of screw speed on the d_{50} and oversized fraction was more pronounced at high L/S ratios. This is illustrated by the interaction plot in Figure 7.

Although the torque was increased by a higher number of kneading elements, no influence of the number of kneading elements on the granule size distribution was detected (Figure 6). This is most remarkable since compaction of the powder mass takes place along the kneading zone and kneading elements favor mixing between the granulation liquid and the powder. Taking into account that the compressive forces at low screw speed due to a high filling degree of the granulator barrel did not favor granule growth either, this confirmed the hypothesis that granule growth of mannitol particles was not caused by compressive forces but rather by formation of liquid and solid bridges after crystallization of solubilized material.

The yield of the granulation process varied between 13 and 56% before milling and was strongly affected by a high oversized fraction (varying between 36 and 86%). Consequently, the process yield was inversely related to the screw speed and L/S ratio (Figure 6).

After milling with a grater screen of 1500 µm, the oversized fraction was eliminated but the fines fraction was generally larger. Nevertheless, the yield of particles suitable for tableting increased after milling and varied between 79 and 89%. No influence of the process parameters on fines and oversized fraction or yield was detected after milling. The d_{50} after milling was only influenced by the L/S ratio (Figure 8). No effect of the screw speed on d_{50} was observed since the oversized fraction, created at high screw speed, was eliminated by milling.

3.2.4. Flowability and friability

The compressibility index (C%) and flowability index (ffc) were influenced by the L/S ratio and screw speed (Figure 9). Increasing the L/S ratio resulted in higher d_{50} values of the milled granules and consequently yielded better flowing granules.

Overall the granules were classified as very cohesive to easy flowing based on their ffc value, and as having a fair to excellent flowability based on the C% value [41].

The friability of the granules ranged from 6.1 to 50.5% and mainly depended on the L/S ratio. At higher L/S ratios more material dissolved in the granulation liquid which formed strong solid bridges after crystallization, resulting in less friable granules. The screw speed had a minor influence on the granule friability (Figure 9). Fewer compaction forces acted on the material at high screw speeds and consequently weaker bonds were formed inside the granules.

3.2.5. Dynamic vapor sorption

Mannitol is considered as a non-hygroscopic excipient [Rowe, Yoshinari2002]. Nevertheless, the hygroscopicity of the granules was investigated by DVS analysis since a strong increase in specific surface area was microscopically observed. Sorption and desorption curves of β- and δ-mannitol starting material, granules derived from β-mannitol starting material (runs 21 and 22) and a selection of representative granules derived from δ-mannitol starting material (runs 14 and 19) are shown in Figure 10. The maximal moisture uptake of β- and δ-mannitol starting material and the granules derived from β-mannitol starting material did not exceed 0.60%, whereas the maximal moisture uptake of the granules derived from δ-mannitol starting material varied between 0.87 and 2.08% (Table 2). The maximal moisture uptake was linked to the percentage of residual δ-mannitol. Granules with a high percentage of residual δ-mannitol (e.g. run 19 in Figure 10) absorbed less moisture compared to samples where the polymorphic transition of δ- to β-mannitol was almost complete (e.g. run 14 in Figure 10). No significant difference in level of hysteresis between sorption and desorption was observed in the samples.

3.3. Influence of the design variables on tablet quality

3.3.1. Tabletability and compression mechanism

The tensile strength (TS) of tablets produced with β- and δ-mannitol reference material and granules manufactured using β-mannitol was compared to the TS of tablets manufactured with granules using δ-mannitol as starting material (Figure 11). The tabletability of four samples (runs 2, 5, 13 and 19) was not investigated as they lacked sufficient flowability for tableting on a rotary tablet press.

These samples were produced at low L/S ratios and at high screw speed, conditions that negatively influenced the flowability (Figure 9).

The tabletability of δ-mannitol reference material was significantly higher than of β-mannitol reference material, reaching a maximal TS of 2.1 MPa. Superior compaction properties of δ-mannitol were also reported by Burger et al., Wagner et al. and Vanhoorne et al. [23, 34, 42]. The TS of granules derived from β-mannitol starting material did not exceed 1.6 MPa and was independent of the applied MCP. However, the tabletability of all granules that used δ-mannitol as starting material underwent a transition to β-mannitol during granulation and their tabletability was significantly enhanced compared to the other test materials. A linear relationship between MCP and TS was observed and maximal TS values of 4.2 - 5.7 MPa were obtained. This was attributed to the polymorphic transition from δ- to β-mannitol during granulation resulting in granules with a specific morphology (aggregates of small needle-shaped primary crystals) and an increased specific surface area. Yoshinari et al. demonstrated that this unique particle structure resulted in enhanced plastic deformability and increased tabletability [22]. No correlation between the investigated properties (e.g. residual percentage of δ-mannitol) of granules derived from δ-mannitol and their tabletability was established. Therefore a full polymorphic transition from δ- to β-mannitol must not be pursued to obtain granules with improved tabletability and that there is no optimum in the ratio of δ-:β-mannitol with regard to tabletability. This was in agreement with the microscopic observations and SSA measurements since the specific morphology (aggregates of small needle-shape primary crystals) and increased SSA were present in all granules derived from δ-mannitol, independently of the percentage residual δ-mannitol in the granules. It was therefore concluded that the specific granule morphology associated with the polymorphic transition was key to the improved tabletability. Moreover the process was considered to be robust since variation in the process parameters could not influence the tabletability.

The compression mechanism of the granules derived from β- and δ-mannitol was also investigated in the current study. Therefore the in-die elastic recovery (IER), plasticity constant (PC) and the elastic energy were calculated based on the energy plots (Table 3). Based on IER and elastic energy, no difference in elastic behavior was detected between β-mannitol granules, β- and δ-mannitol reference material. However, granules derived from δ-mannitol and δ-mannitol reference material exhibited higher plasticity constants than granules derived from β-mannitol or β-mannitol reference material. Therefore it was concluded that the superior tabletability of granules derived from δ-mannitol over granules derived from

β-mannitol was due to better plastic deformation characteristics of the former. This confirmed the research of Yoshinari et al. [22].

3.3.2. Friability

The friability of tablets produced with granules of runs 1 - 20 (δ-mannitol starting material) and with δ-mannitol reference material was lower than 1%. In contrast, granulation with β-mannitol starting material resulted in highly friable tablets (4.7 and 21.5% for runs 21 and 22, respectively). This confirmed the tabletability experiments as the enhanced plastic deformation of granules derived from δ-mannitol resulted in tablets with a higher tensile strength and lower friability. The friability of tablets with β-mannitol starting material was excessively high as these tablets completely fragmented during friability testing.

3.4. Stability

Samples of the unmilled granules were stored at 25 °C / 40% RH and at 40 °C / 75% RH. They were analyzed by Raman spectroscopy after 6 months and the percentage δ-mannitol was calculated by the PLS model (Table 2). After storage a lower amount of δ-mannitol was found in all samples, irrespectively of the storage conditions. However, a significant decrease in the percentage of residual δ-mannitol was only detected in three samples (runs 5, 13, 19) after storage at 40 °C / 75% RH. These samples were produced at a low L/S ratio and a high screw speed and contained a relatively large fraction of residual δ-mannitol. The limited moisture uptake during storage at higher RH apparently induced a further moisture-mediated transition from δ- to β-mannitol. Hence, storage at lower RH is preferred to avoid polymorphic transition.

4. Conclusions

A different granulation behavior of mannitol was identified during continuous twin-screw granulation compared to other commonly used excipients such as lactose and MCC as the effect of granulation parameters (filling degree, screw speed, number of kneading elements) on the granule size distribution of mannitol granules was different compared to literature reports on formulations containing lactose and/or MCC as filler. Based on the higher solubility and faster

dissolution rate of mannitol it was concluded that granulation of mannitol was principally driven by formation of liquid and solid bridges of solubilized material, rather than by compressive forces in the granulator barrel.

A polymorphic transition of mannitol was reported during twin screw granulation, which allowed to improve the tabletability of this material. Despite the short residence times and low L/S ratios used in twin screw granulation in comparison to batch granulation, the polymorphic transition of δ- to β-mannitol was observed, yielding a unique granule morphology with a higher specific surface area and enhanced plastic deformability. The superior tabletability of these granules derived from δ-mannitol as starting material over granules derived from β-mannitol as starting material was attributed to this unique granule morphology which was not dependent on the process parameters. Therefore the process was considered as robust. The excellent tabletability of granules derived from δ-mannitol is promising and its potential in combination with highly dosed poorly compressible drugs will be investigated in a next study.

Acknowledgement

The authors would like to acknowledge Merck (Darmstadt, Germany) for supplying δ-mannitol.

References

[1] K. T. Lee, A. Ingram, N. A. Rowson, Comparison of granule properties produced using Twin Screw Extruder an High Shear Mixer: A step towards understanding the mechanism of twin screw wet granulation, Pow. Tech. 238 (2013) 91-98.

[2] C. Vervaet, J.P. Remon, Continuous granulation in the pharmaceutical industry, Chem. Eng. Sci 60 (2005) 3949-3957.

[3] P. Hurter, H. Thomas, D. Nadig, D. Emiabata-Smith, A. Paone, Implementing continuous manufacturing to streamline and accelerate drug development, AAPS news magazine (Augustus 2013) 15-19.

[4] W. De Soete, J. Dewulf, P. Cappuyns, G. Van der Vorst, B. Heirman, W. Aelterman, K. Schoeters, H. Van Langenhove, Exergetic sustainability assessment of batch versus continuous wet granulation based pharmaceutical tablet manufacturing: a cohesive analysis at three different levels, Green Chem. 15 (2013) 3001-3278.

[5] W. D. Tu, A. Ingram, J. Seville, Regime map development for continuous twin screw granulation, Chem. Eng. Sci 87 (2013) 315-326.

[6] A. Kumar, M. Alakarjula, V. Vanhoorne, M. Toiviainen, F. De Leersnyder, J. Vercruysse, M. Juuri, J. Ketolainen, C. Vervaet, K.V. Gernaey, T. De Beer, I. Nopens, Experimental investigation linking granulation performance with

[7] J. Vercruysse, D. Córdoba Díaz, E. Peeters, M. Fonteyne, U. Delaet, I. Van Assche, T. De Beer, J. P. Remon, C. Vervaet, Continuous twin screw granulation: Influence of process variables on granule and tablet quality, Eur. J. Pharm. Biopharm. 82 (2012) 205-211.

[8] R.M. Dhenge, R.S. Fyles, J.J. Cartwright, D.G. Doughty, M.J. Hounslow, A.D. Salman, Twin screw wet granulation: Granule properties, Chem. Eng. J. 164 (2010) 322-329.

[9] R.M. Dhenge, J.J. Cartwright, D.G. Doughty, M.J. Hounslow, A.D. Salman, Twin screw granulation: Effect of powder feed rate, Adv. Powder Technol. 22 (2011) 162-166.

granulation, Eur. J. Pharm. Biopharm. in press, doi: 10.1016/j.ejps.2015.12.021
residence time and granulation liquid distributions in twin-screw
[10] D. Djuric, P. Kleinebudde, Impact of Screw Elements on Continuous Granulation With a Twin-Screw Extruder, J. Pharm. Sci. 97 (2008) 4934-4942.
[11] D. Djuric, P. Kleinebudde, Continuous granulation with a twin-screw extruder: Impact of material throughput, Pharm. Dev. Technol. 15 (2010) 518-525.
[12] M.R. Thompson, J. Sun, Wet granulation in a twin-screw extruder: implications of screw design, J. Pharm. Sci 99 (2010) 2090-2103.
[13] E. I. Keleb, A. Vermeire, C. Vervaet, J. P. Remon, Single-step granulation/tabletting of different grades of lactose: a comparison with high shear granulation and compression, Eur. J. Pharm. Biopharm. 58 (2004) 77-82.
[14] J. Vercruysse, A. Burggraeve, M. Fonteyne, P. Cappuyns, U. Delaet, I. Van Assche, T. De Beer, J.P. Remon, C. Vervaet, Impact of screw configuration on the particle size distribution of granules produced by twin screw granulation, Int. J. Pharm. 479 (2015) 171-180.
[15] K.E. Rocca, S. Weatherley, P.J. Sheskey, M.R. Thompson, Influence of filler selection on twin screw foam granulation, Drug Dev. Ind. Pharm. 41 (2015) 35-42.
[16] M. Fonteyne, H. Wickström, E. Peeters, J. Vercruysse, H. Ehlers, B. Peters, J.P. Remon, C. Vervaet, J. Ketolainen, N. Sandler, J. Rantanen, K. Naelapää, T. De Beer, Influence of raw material properties upon critical quality attributes of continuously produced granules and tablets, Eur. J. Pharm. Biopharm. 87 (2014) 252-263.
[17] L. Tan, A.J. Carella, Y. Ren, J.B. Lo, Process optimization for continuous extrusion wet granulation, Pharm. Dev. Technol. 16 (2011) 302-315.
[18] M.R. Thompson, S. Weatherley, R.N. Pukadyil, P.J. Sheskey, Foam granulation: new developments in pharmaceutical solid oral dosage forms using twin screw extrusion machinery, Drug Dev. Ind. Pharm. 38 (2012) 771-784.

[19] A.S. El Hagrasy, J.R. Hennenkamp, M.D. Burke, J.J. Cartwright, J.D. Litster, Twin screw wet granulation: Influence of formulation parameters on granule properties and growth behavior, Powder Technol. 238 (2013) 108-115.

[20] S. Yu, G.K. Reynolds, Z. Huang, M. de Matas, A.D. Salman, Granulation of increasingly hydrophobic formulations using a twin screw granulator, Int. J. Pharm. 475 (2014) 82-96.

[21] W.L. Hulse, R.T. Forbes, M.C. Bonner, M. Getrost, The characterization and comparison of spray-dried mannitol samples, Drug Dev. Ind. Pharm. 35 (2009) 712-718.

[22] T. Yoshinari, R. T. Roberts, P. York, Y. Kawashima, The improved compaction properties of mannitol after a moisture-induced polymorphic transition, Int. J. Pharm. 258 (2003) 121-131.

[23] C.M. Wagner, M. Pein, J. Breitkreutz, Roll compaction of granulated mannitol grades and the unprocessed crystalline delta-polymorph, Pow. Tech. 270 (2015) 470-475.

[24] R. C. Rowe, P.J.S. Sheskey, S.C. Owen, Handbook of pharmaceutical excipients, 2006 449-453.

[25] Commercial information provided by Merck, available via http://85.238.144.18/lifescience/literature/Parteck%20Delta%20M.pdf

[26] A. Kumar, J. Vercruysse, M. Toiviainen, P.E. Panouillot, M. Juuti, V. Vanhoorne, K.V. Gernaey, T. De Beer, I. Nopens, Mixing and transport during pharmaceutical twin-screw wet granulation: experimental analysis via chemical imaging 87 (2014) 279-289.

[27] R.M. Dhenge, J.J. Cartwright, M.D. Hounslow, A.D. Salman, Twin screw granulation: effects of properties of granulation liquid, Pow. Tech. 229 (2012) 126-136.

[28] P. Beer, D. Wilson, Z. Huang, M. De Matas, transfer from high-shear batch to continuous twin screw wet granulation: a case study in understaning the relationship between process parameters and product quality attributes, J. Pharm. Sci. 103 (2014) 3075-2082.

[29] E. I. Keleb, A. Vermeire, C. Vervaet, J. P. Remon, Continuous twin screw extrusion for the wet granulation of lactose, Int. J. Pharm. 239 (2002) 69-80.

[30] T.R.M. De Beer, M. Alleso, F. Goethals, A. Coppens, Y. Vander Heyden, H. Lopez De Diego, J. Rantanen, F. Verpoort, C. Vervaet, J.P. Remon, W.R.G. Baeyens, Implementation of a process analytical technology system in a freeze-drying process using raman spectroscopy for in-line process monitoring, Anal. Chem 79 (2007) 7992-8003

[31] J. T. Fell, J. M. Newton, The tensile strength of lactose tablets, J. Pharm. Pharmacol. 20 (1968) 658-675.

[32] N. A. Armstrong, R. F. Haines-Nutt, Elastic recovery and surface area changes in compacted powder systems. J. Pharm. Pharmacol. 24 (1972) 135–136.

[33] M. R. Thompson, Twin screw granulation – review of current progress, Drug Dev. Ind. Pharm. 41 (2015) 1223-1231.

[34] A. Burger, J. Henck, S. Hetz, J.M. Rollinger, A.A. Weissnicht, H. Stöttner, Energ/Temperature diagram and compression behavior of the polymorphs of D-mannitol, J. Pharm. Sci. 89 (2000) 457-468.

[35] T. Yoshinari, R. T. Roberts, P. York, Y. Kawashima, Moisture induced polymorphic transition of mannitol and its morphological transition, Int. J. Pharm. 247 (2002) 69-77.

[36] J. Cornel, P. Kidambi, M. Mazzotti, Precipitation and transformation of the three polymorphs of D-mannitol, Ind. Eng. Chem. Res. 49 (2010) 5854-5862.

[37] S. N. Campbell Roberts, A. C. Williams, I. M. Grimsey, S. W. Booth, Quantitative analysis of mannitol polymorphs. X-ray powder diffractometry – exploring preferred orientation effects, J. Pharm. Biomed. Anal. 28 (2002) 1149-1159.

[38] M. Inoue, I. Hirasawa, The relationship between crystal morphology and XRD peak intensity on $CaSO_4.2H_2O$, J. Cryst. Growth 380 (2013) 169-175.

[39] R. M. Dhenge, J. J. Cartwright, M. J. Hounslow, A. D. Salman, Twin screw granulation: Steps in granule growth, Int. J. Pharm. 438 (2012) 20-32.

[40] E. I. Keleb, A. Vermeire, C. Vervaet, J. P. Remon, Twin screw granulation as a simple and efficient tool for continuous wet granulation, Int. J. Pharm. 273 (2004) 183-194.

[41] D. Schulze, Powders and bulk solids, Springer Verlag Berlin Heidelberg, 2008, pp. 42.

[42] V. Vanhoorne, P. J. Van Bockstal, B. Van Snick, E. Peeters, T. Monteyne, P. Gomes, T. De Beer, J. P. Remon, C. Vervaet, Continuous manufacturing of delta mannitol by cospray drying with PVP, Int. J. Pharm. 501 (2016) 139-147.

Tables

Table 1: Overview of the granulation experiments.

Run	L/S ratio	Temperature (°C)	Screw speed	Number of kneading elements	Starting material
1	0.12	32.5	650	12	δ-mannitol
2	0.08	40	900	12	δ-mannitol
3	0.08	40	400	12	δ-mannitol
4	0.08	25	400	12	δ-mannitol
5	0.08	25	900	12	δ-mannitol
6	0.16	25	900	12	δ-mannitol
7	0.16	25	400	12	δ-mannitol
8	0.16	40	400	12	δ-mannitol
9	0.16	40	900	12	δ-mannitol
10	0.12	32.5	650	12	δ-mannitol
11	0.12	32.5	650	6	δ-mannitol
12	0.08	25	400	6	δ-mannitol
13	0.08	25	900	6	δ-mannitol
14	0.16	25	400	6	δ-mannitol
15	0.16	25	900	6	δ-mannitol
16	0.16	40	900	6	δ-mannitol
17	0.16	40	400	6	δ-mannitol
18	0.08	40	400	6	δ-mannitol
19	0.08	40	900	6	δ-mannitol
20	0.12	32.5	650	6	δ-mannitol
21	0.16	25	400	12	β-mannitol
22	0.08	25	900	6	β-mannitol

Table 2 Overview of the percentage δ-mannitol in the unmilled and milled granules and unmilled granules after 6 months storage (25 °C and 40% RH or 40 °C and 75% RH), the maximal moisture content absorbed during DVS analysis and the specific surface area.

Run	% δ-mannitol before milling	% δ-mannitol after milling	% δ-mannitol after 6 months at 25 °C and 40% RH	% δ-mannitol after 6 months at 40 °C and 75% RH	Moisture content at 95% RH (%)	Specific surface area (m^2/g)
1	10	7	6	7	1.87	-[c]
2	14	12	9	9	1.54	-[c]
3	9	9	6	7	1.84	-[c]
4	10	9	7	6	1.84	1.7620
5	23	26	26	12	2.08	-[c]
6	8	8	5	6	1.81	-[c]
7	-[a]	-[a]	-[a]	-[a]	-[a]	-[c]
8	6	-[b]	3	6	-[c]	-[c]
9	7	5	4	6	1.74	1.4312
10	9	6	4	6	1.80	1.1167
11	14	10	8	9	1.18	-[c]
12	15	16	11	10	1.27	-[c]
13	31	28	24	13	0.87	-[c]
14	8	8	4	6	1.83	-[c]
15	15	13	10	10	1.57	-[c]
16	13	9	10	11	1.48	-[c]
17	9	8	6	6	1.83	1.0907
18	19	20	15	10	1.40	2.4289
19	45	40	39	13	1.34	1.7945
20	13	14	10	10	1.33	2.0907
21	6	-[d]	4	-[c]	0.43	-[c]

22	6	-[d]	4	-[c]	0.56	0.2346
β-mannitol reference	-[c]	-[c]	-[c]	-[c]	0.26	0.1355
δ-mannitol reference	-[c]	-[c]	-[c]	-[c]	0.60	0.5169

[a]Run 7 was eliminated from the experimental design because of too high torque values immediately after start-up.
[b]The amount of granules collected was too limited to mill the samples.
[c]No data collected.

Table 3 Overview of in-die elastic recovery (IER), plasticity constant (PC) and elastic energy (E)..

run	IER (%)	PC	elastic E (J)
1	2.6	93.3	0.5
3	3.1	92.1	0.6
4	2.8	92.8	0.5
6	2.9	93.3	0.5
9	2.5	93.2	0.5
10	3.0	93.1	0.6
11	3.4	94.2	0.4
12	2.4	94.1	0.4
14	3.0	92.4	0.5
15	2.3	94.6	0.4
16	3.0	92.4	0.5
17	2.5	92.2	0.4
18	2.4	94.0	0.5
20	2.9	94.2	0.4
21	2.3	89.0	0.4
22	2.7	91.2	0.5
β-mannitol reference	2.9	90.0	0.5
δ-mannitol reference	2.2	94.0	0.4

Figures

Figure 1 Energy plot of punch stroke against compression force for β-mannitol reference material compressed at 150 MPa.

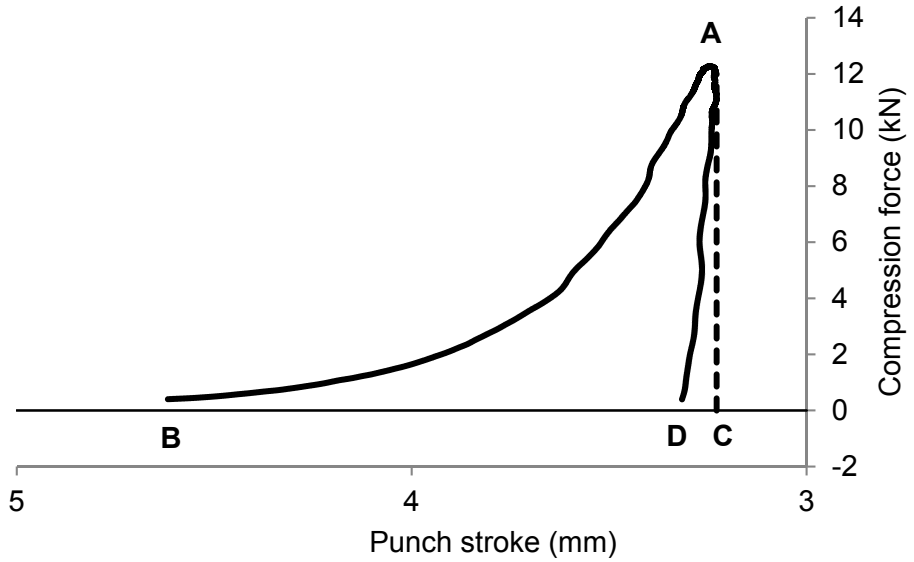

Figure 2 Effect plot showing the influence of the process parameters on torque.

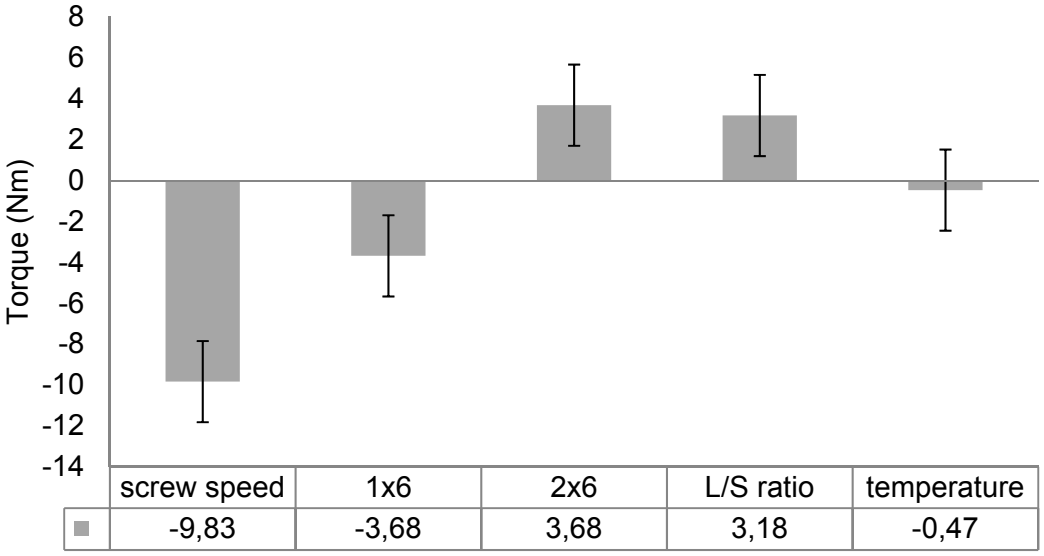

Figure 3 Effect plot showing the influence of the process parameters on the percentage residual δ-mannitol in the granules before (top) and after milling (bottom).

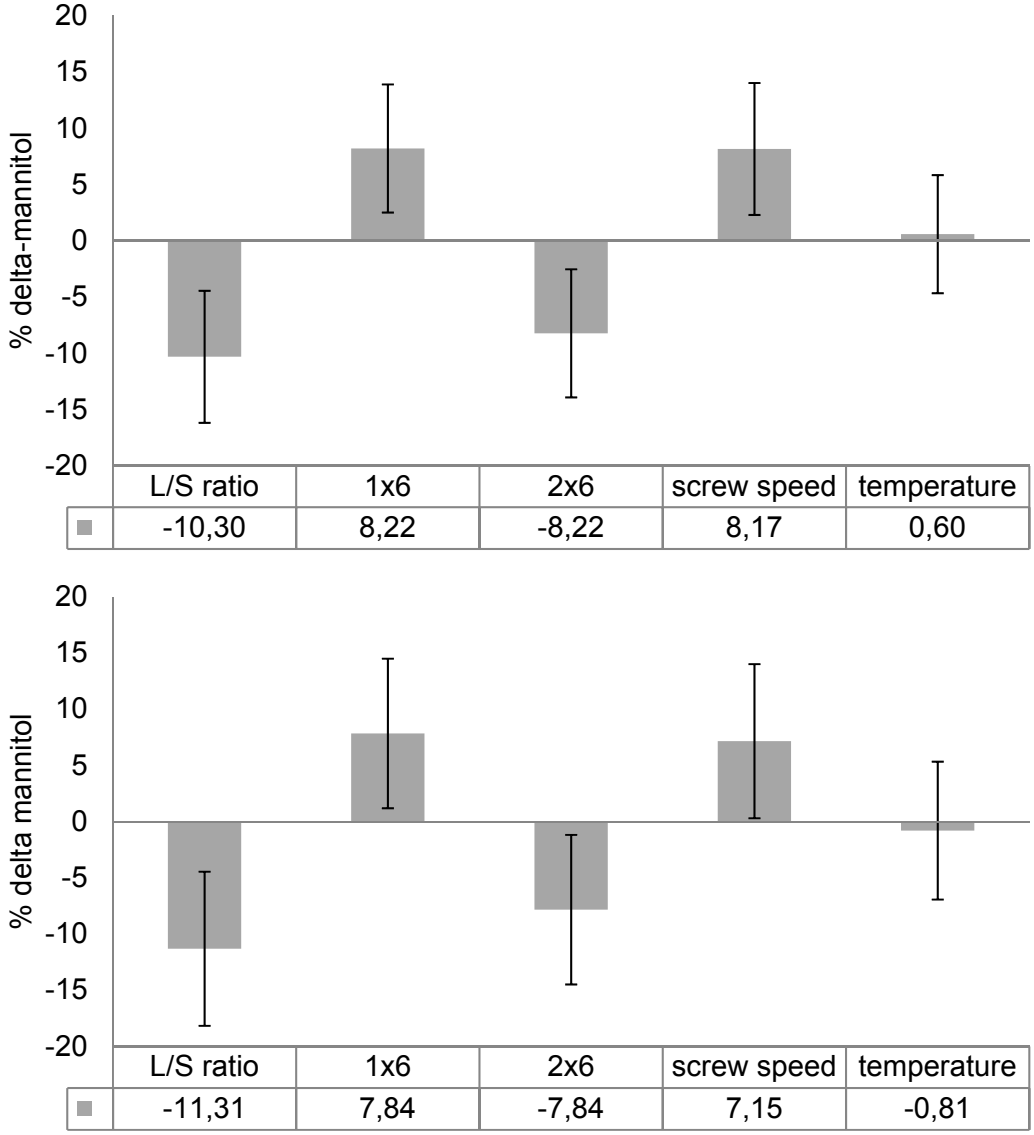

Figure 4 XRD patterns of reference material of α-, β- and δ-mannitol and runs 1-20.

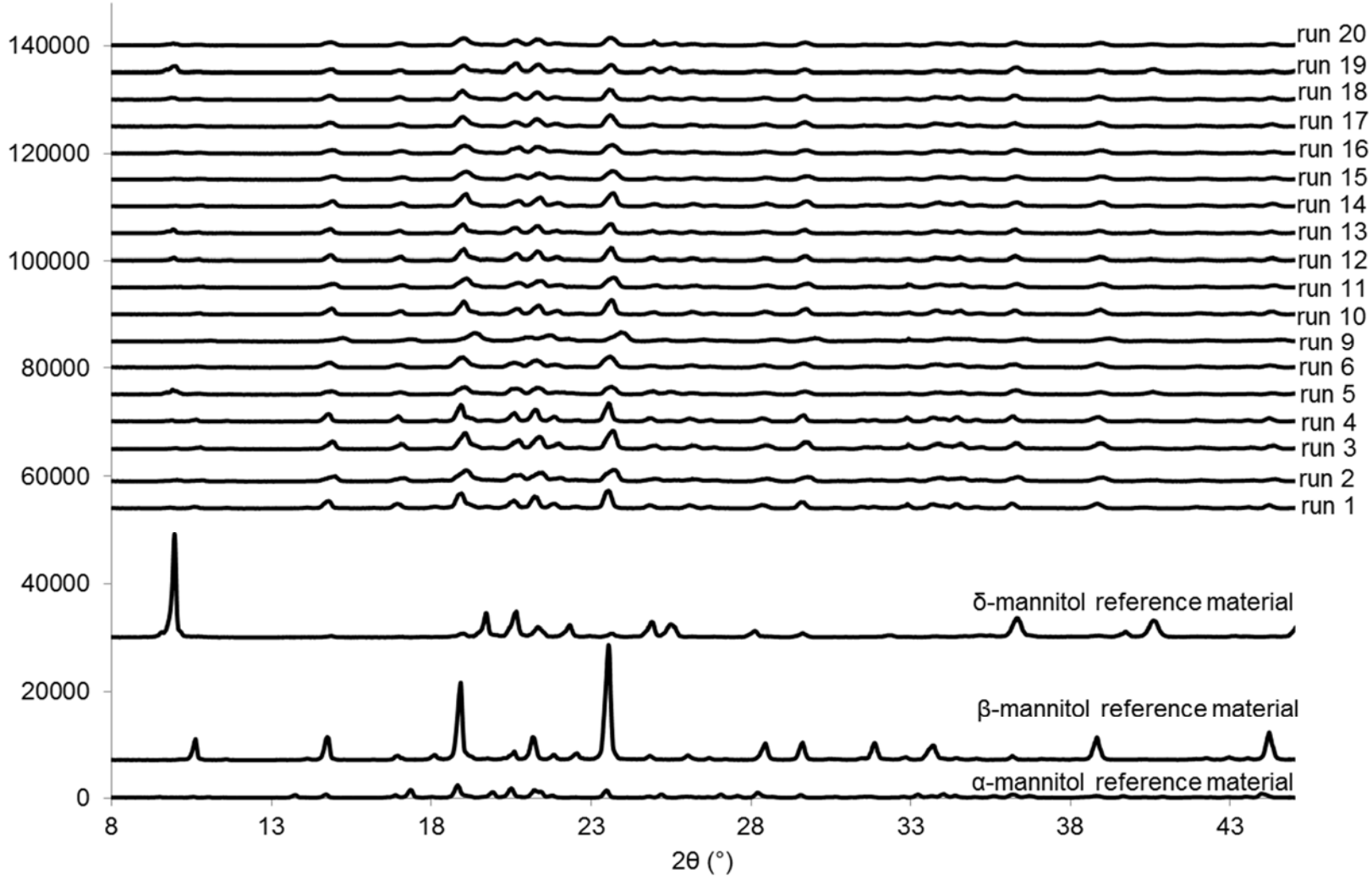

Figure 5 SEM images of β- and δ-mannitol reference material and representative samples of granulated β-mannitol (runs 21 and 22) and of granulated δ-mannitol (runs 14, 19).

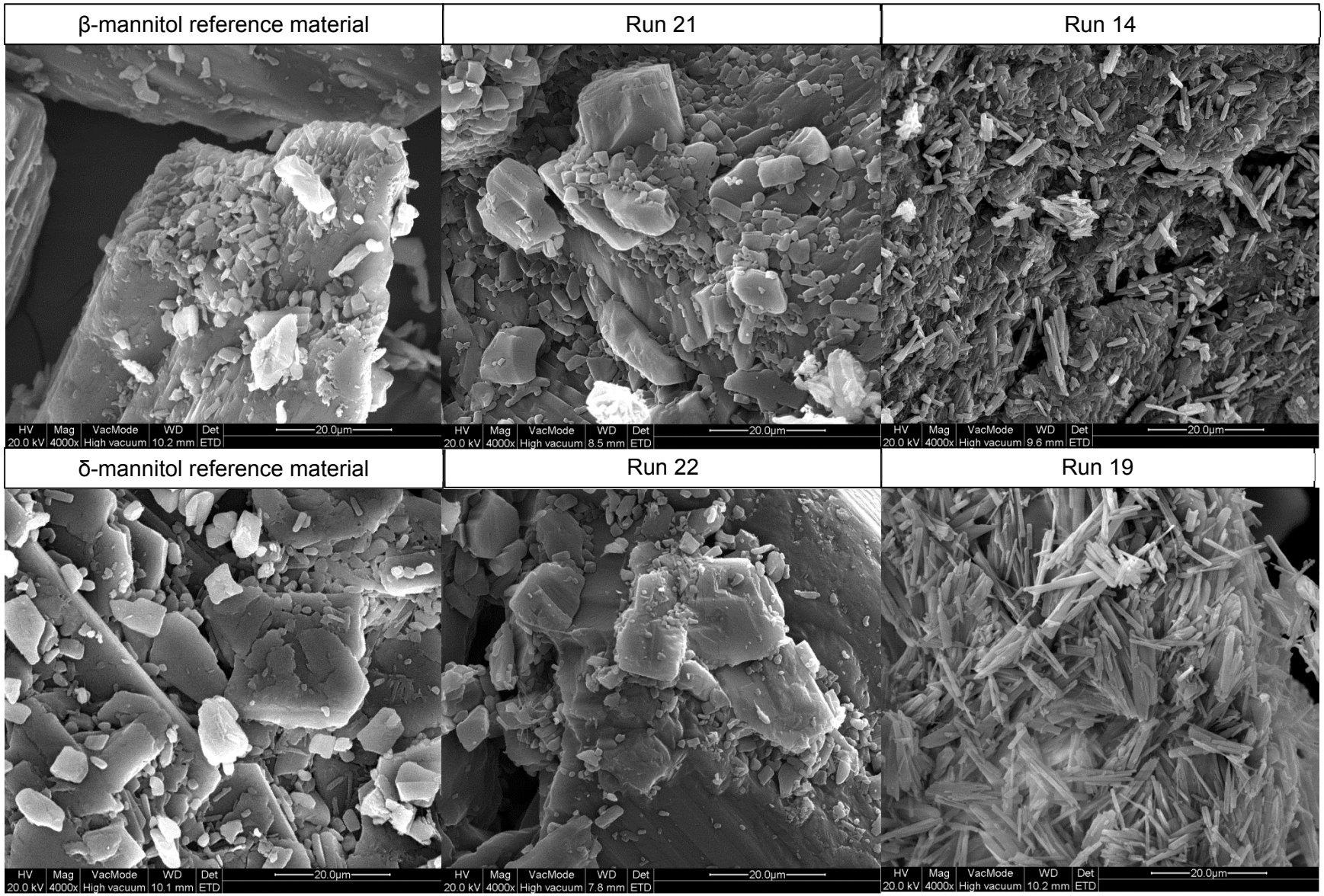

Figure 6 Effect plots visualizing the influence of the process parameters on d_{50} (A), yield (B), fines (C) and oversized fraction (D) of the granules before milling.

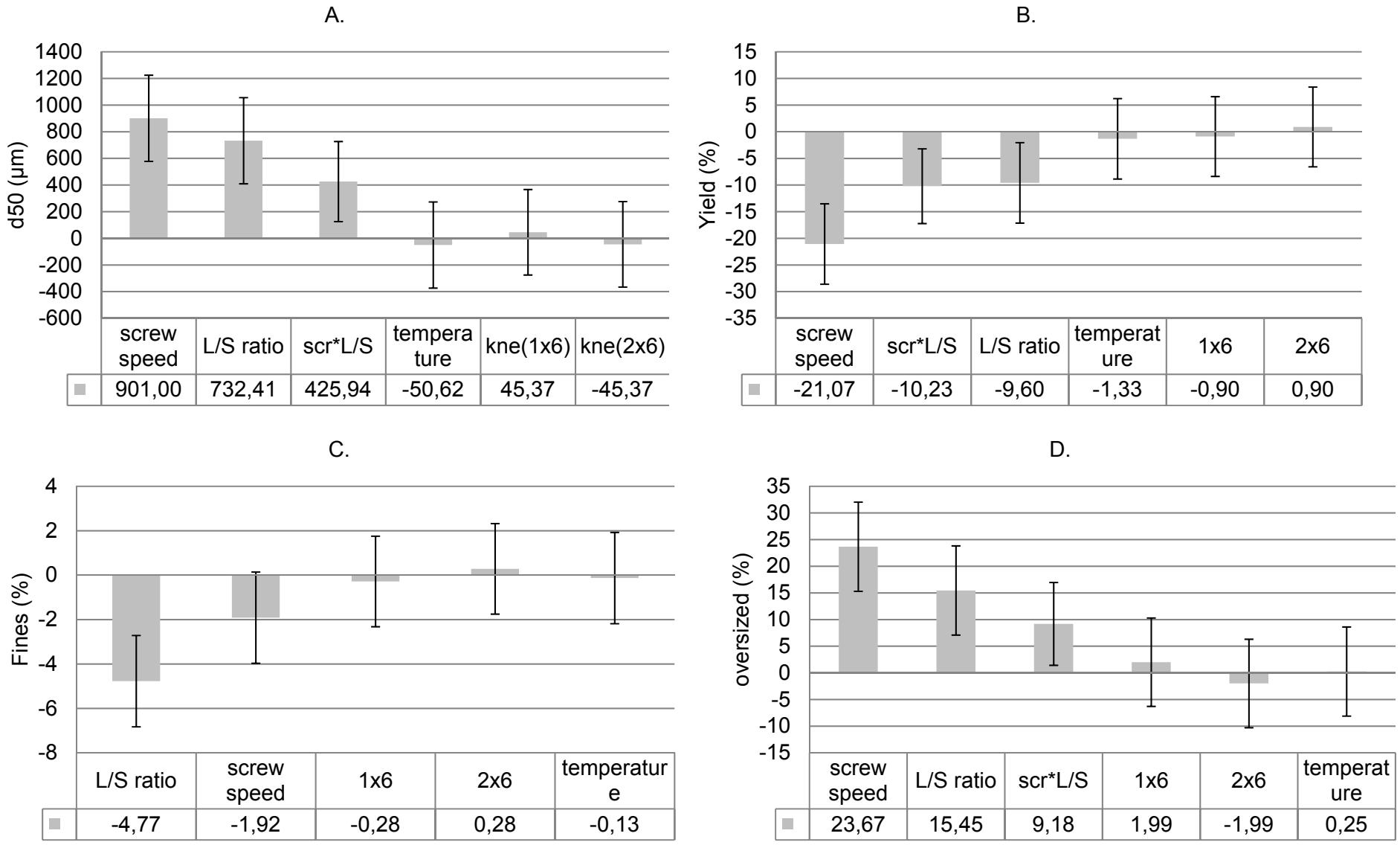

Figure 7 Interaction plots showing the combined effect of the L/S ratio (full line: L/S = 0.16 and dotted line: L/S = 0.08) and screw speed on the d_{50} (A), yield (B) and the fraction of oversized granules (C).

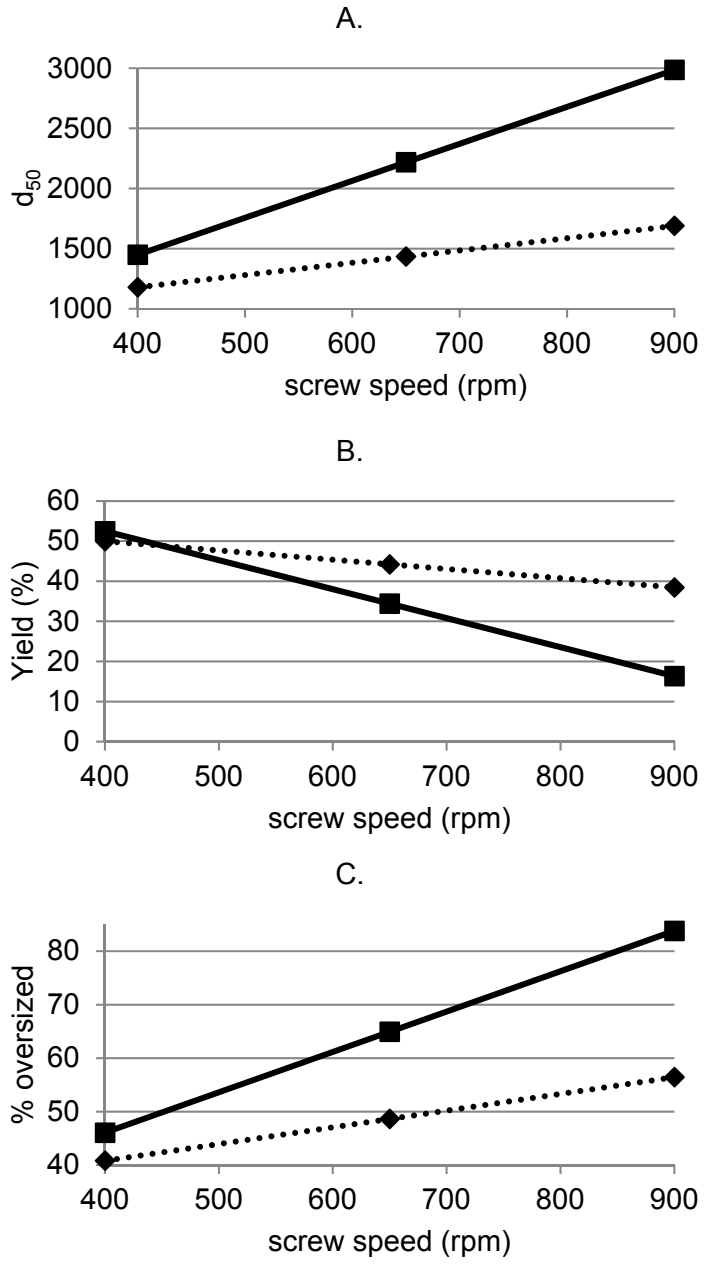

Figure 8 Effect plots visualizing the influence of the process parameters on d_{50} (A), yield (B), fines (C) and oversized fraction (D) of the granules after milling.

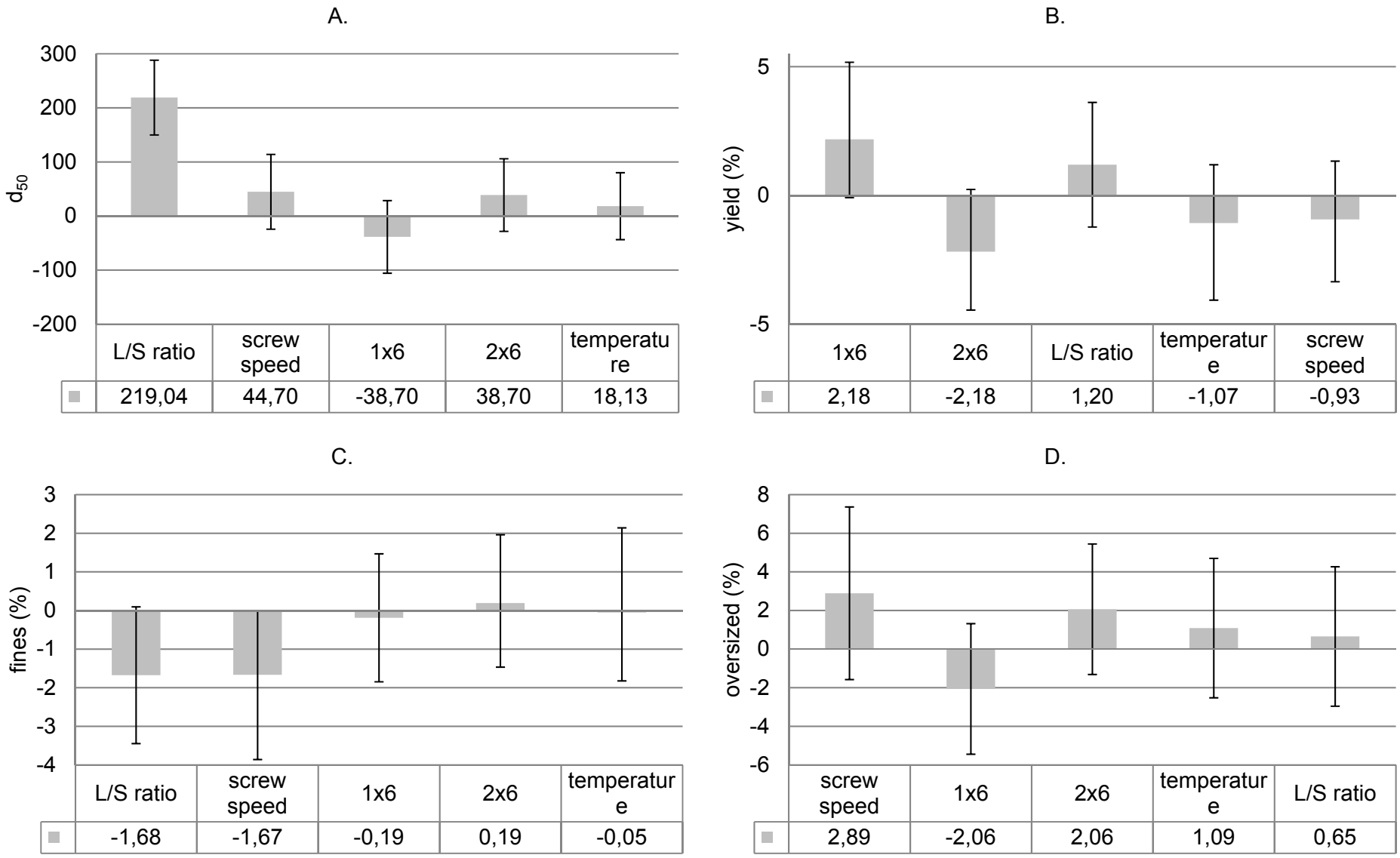

Figure 9 Effect plots visualizing the influence of the process parameters on compressibility index (C%) (A), flowability index (ffc) (B) and granule friability (C).

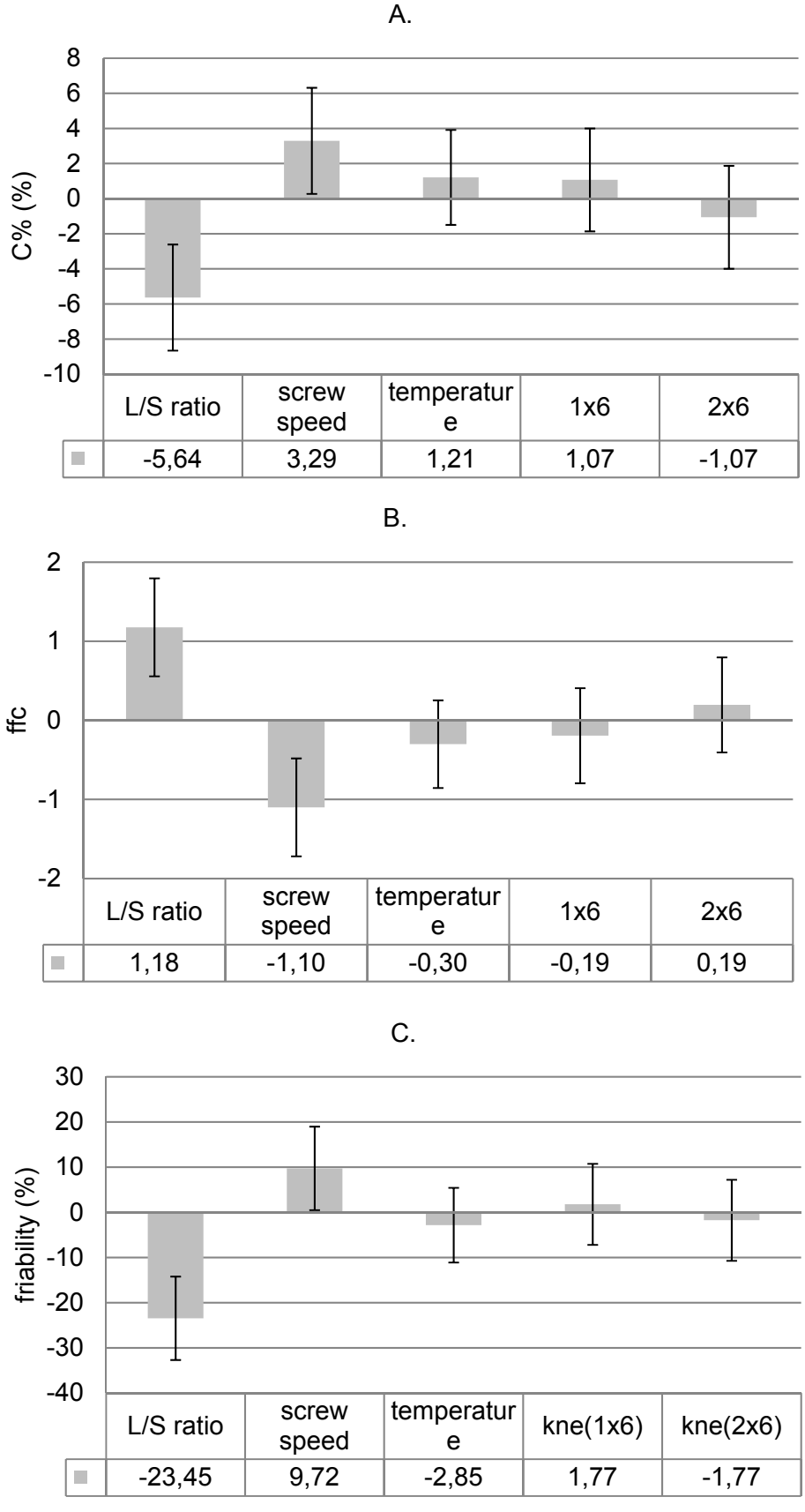

Figure 10 DVS sorption and desorption curves of β-mannitol (full black line) and δ-mannitol (dotted black line) reference material, granulated β-mannitol samples 21 (full grey line) and 22 (dotted grey line) and granulated δ-mannitol samples 14 (full blue line) and 19 (full green line).

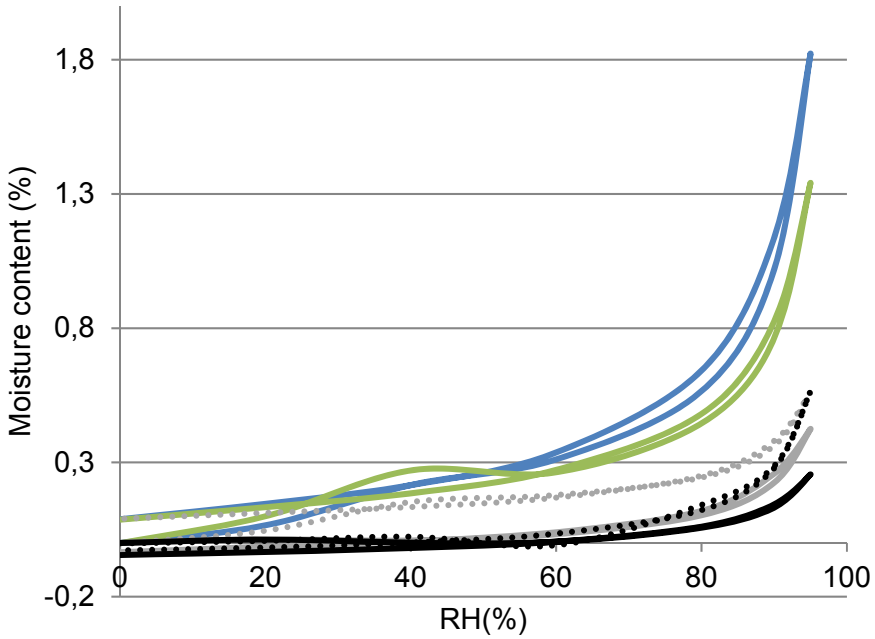

Figure 11 Tabletability of β- and δ-mannitol reference material, granulated β-mannitol (run 21 and 22) and granulated δ-mannitol samples.